

## A Photographic System for the Three-Dimensional Study of Facial Morphology

Marcio de Menezes<sup>a</sup>; Riccardo Rosati<sup>a</sup>; Cristina Allievi<sup>a</sup>; Chiarella Sforza<sup>b</sup>

### ABSTRACT

**Objectives:** To test whether digital photographs supported by three-dimensional (3D) software are suitable for measuring the facial soft tissues of healthy subjects as compared with data obtained by a certified 3D computerized electromagnetic digitizer.

**Materials and Methods:** Three-dimensional soft tissue facial landmarks were obtained from the faces of 15 healthy young adults, using a 3D computerized electromagnetic digitizer and a new low-cost photogrammetry system. Twelve linear and 18 angular measurements were computed. Errors between methods and repeatability of the new method were calculated.

**Results:** Systematic errors between methods were found for only two distances and three angles (paired *t*-test,  $P < .05$ ). The mean absolute differences between methods were always lower than 3 mm and 3 degrees. Repeated digitization of photographs showed that the method was repeatable (no systematic differences; random errors lower than 1.6 mm and 3 degrees). Repeated sets of photographs showed random errors of up to 5.3 mm and 5.6 degrees, without systematic biases.

**Conclusion:** The 3D photogrammetry system can provide reliable facial measurements. The method is relatively fast and requires only inexpensive equipment. It is simple to use for private practice, research, or other practice. (*Angle Orthod.* 2009;79:1070–1077.)

**KEY WORDS:** Face; Soft tissue analysis; Three-dimensional; Photographs

### INTRODUCTION

Accurate facial analysis is essential for diagnosis and preparation of a treatment plan for patients undergoing orthodontic treatment, orthognathic surgery, or facial plastic surgery; for diagnosis of genetic and acquired malformations; for the study of normal and abnormal growth; and for morphometric investigation.<sup>1–5</sup> Because facial anthropometry plays an important role in the diagnosis of several dysmorphic syndromes,<sup>2,4–8</sup> clinicians should apply the best diagnostic techniques for patient education, presurgical planning, and postoperative analysis.

With constant upgrading of informatics and com-

munication technology, the standards for data storage and retrieval and information usage, allied with biomedical knowledge, have transformed traditional methods of diagnosis, visualization, and treatment.<sup>2,4,8–13</sup> These efforts were aimed at reducing the time spent on examinations and improving the reliability of measurements.

Different modalities of diagnosis and treatment control with the use of images for anthropometric evaluation developed over the years include two-dimensional (2D) photography and three-dimensional (3D) reconstruction. 2D photography offers rapid capture of facial images, almost permanent retention, and the opportunity for repeated measurement, but single 2D images are affected adversely by projection, distortion, and pose.<sup>1,3,7,8,12,14,15</sup>

As recently reviewed,<sup>16,17</sup> the development of different techniques for 3D reproduction of facial topography such as ultrasound, laser scanning, holography, computed tomography (CT), magnetic resonance (MR), electromagnetic digitizer, and stereophotogrammetry, significantly changed the process of diagnosis by providing a lot of facial anatomical details.<sup>1,3–5,7,8,11–13,18–21</sup> Three-dimensional reconstruction,

<sup>a</sup> Postgraduate student, Department of Human Morphology, University of Milan, Milano, Italy.

<sup>b</sup> Professor, Department of Human Morphology, University of Milan, Milano, Italy.

Corresponding author: Dr Chiarella Sforza, Department of Human Morphology, via Mangiagalli 31, University of Milan, Milano, MI I-20133 Italy (e-mail: chiarella.sforza@unimi.it)

Accepted: January 2009. Submitted: November 2008.

© 2009 by The EH Angle Education and Research Foundation, Inc.

which has the potential to compensate for the inadequacies of a 2D image, has great potential for the diagnosis of patient abnormalities and for syndrome delineation.<sup>1,7,8,15,21</sup>

Unfortunately, current devices for facial 3D analysis are costly, impeding their routine clinical use. Additionally, they often need dedicated spaces, which cannot be organized within dental and orthodontic offices, thus limiting the use of 3D analysis to university laboratories and research centers.<sup>2,15,20</sup>

As the use of digital photography and computer imaging increases, morphometric evaluation must become a simple and cost-effective method to assess soft tissue changes in a reliable way.<sup>2,9,20</sup> The aim of this study was to test whether digital facial photographs supported by a commercial 3D software program are suitable for measuring the soft tissues of healthy subjects when compared with data obtained by a certified 3D computerized electromagnetic digitizer.<sup>22,23</sup>

## MATERIALS AND METHODS

A convenience group of 15 healthy volunteers, 11 men and 4 women, ranging in age from 22 to 28 years, was included in this study. None of the volunteers had undergone previous facial surgery or had a history of craniofacial trauma or congenital anomalies. All procedures were noninvasive and were carried out with minimal disturbance to the subjects. The local ethics committee approved the protocol, which did not include dangerous or painful procedures. Sample size was chosen with consideration for mean differences between different methods of 1 mm/degree (standard deviation [SD], 0.5), as found in previous studies,<sup>5,20</sup> with  $\alpha = .05$ , and  $\beta = .9$ .

Fifty soft tissue landmarks were considered<sup>23</sup> (Figure 1, Table 1). Although subjects sat in a position suitable for correct identification of facial features, most of the 50 soft tissue facial landmarks,<sup>1,3,4,16,22</sup> except for the inferior and superior points of the nostril axis (Itn; Stn), exocanthion (Ex), endocanthion (En), stomion (Sto), and cheilion (Ch), were marked on the face with black liquid eye liner. The reproducibility of landmark identification was reported previously and was found to be reliable.<sup>22,23</sup> Landmark marking for each subject took less than 5 minutes.<sup>22</sup>

Coordinates of the facial landmarks were collected by two different methods: a 3D computerized electromagnetic digitizer, and a simplified photogrammetry method (PhotoModeler Pro, EOS Systems Inc, Vancouver, British Columbia, Canada). To assess whether measurements provided by the photogrammetry surface imaging system were comparable with those pro-

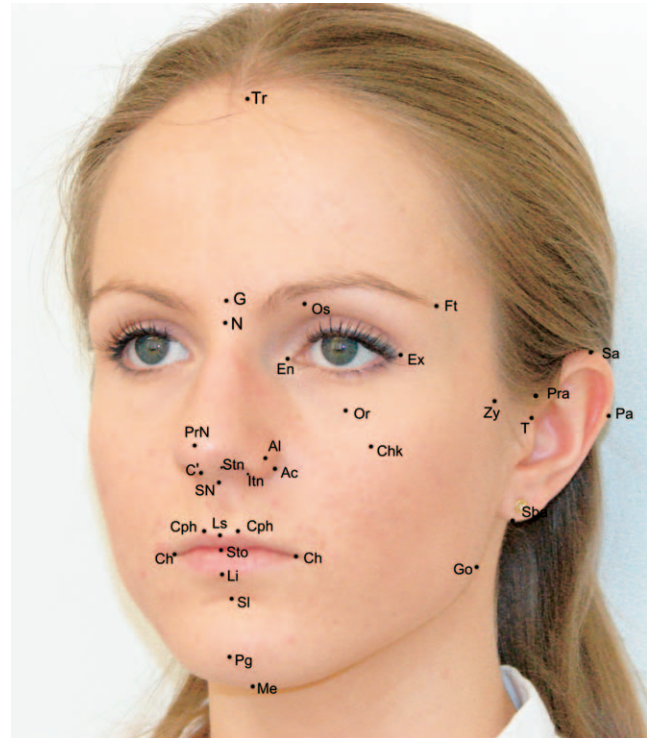


Figure 1. Soft tissue facial landmarks digitized on all subjects.

vided by the electromagnetic digitizer, we computed the same distances and angles by both methods.

### 3D Computerized Electromagnetic Digitizer (Polhemus)

Three-dimensional ( $x, y, z$ ) coordinates of the facial landmarks were obtained with a 3D computerized electromagnetic digitizer (3Draw, Polhemus, Colchester, VT). Using the instrument stylus, a single operator digitized the marked landmarks while subjects sat motionless with a natural head position. Digitization was performed for each subject in less than 60 seconds.

The files of the 3D coordinates were used for all subsequent off-line computerized calculations,<sup>22,23</sup> based on Euclidean geometry (Figure 2). The ( $x, y, z$ ) coordinates of the landmarks obtained for each subject were used to calculate a set of facial angles and distances (Table 2). A detailed description of the procedure can be found elsewhere.<sup>22,23</sup>

The reproducibility of landmark identification and marker positioning has been reported previously and has been found to be reliable, with technical errors of measurement on 50 landmarks of 1.20 mm for males and 0.95 mm for females, equivalent to 1.04% and 1.05% of the relevant nasion–mid-tragion distances.<sup>22</sup>

### Photogrammetry Surface Imaging System (PhotoModeler)

For each subject, three separate, single photographic images (Figure 3) were taken from different

**Table 1.** Digitized facial landmarks and relevant definitions

Midline landmarks:		
Tr	trichion	on the hairline in the middle of the forehead
G	glabella	the most prominent midline point between the eyebrows
N	nasion	the innermost point between forehead and nose
Prn	pronasale	most protruded point of the nasal apex
C'	columella	midpoint between the columella crests
Sn	subnasale	midpoint at the union of the lower border of the nasal septum and the upper lip
Ls	labiale superius	midpoint of the vermilion line of the upper lip
Sto	stomion	midpoint of the horizontal labial fissure
Li	labiale inferius	midpoint of the vermilion line of the lower lip
Sl	sublabiale	in the midline of the nasolabial sulcus
Pg	pogonion	most anterior point of the chin
Me	menton	lowest median point on the lower border of the mandible
Paired landmarks (right and left side noted , and ):		
Ex <sub>r</sub> , Ex <sub>i</sub>	exocanthion	external commissura of the eye fissure
En <sub>r</sub> , En <sub>i</sub>	endocanthion	internal commissura of the eye fissure
Os <sub>r</sub> , Os <sub>i</sub>	orbitale superius	highest point on the lower border of the eyebrow
Or <sub>r</sub> , Or <sub>i</sub>	orbitale	lowest point on the inferior margin of the orbit
Ft <sub>r</sub> , Ft <sub>i</sub>	frontotemporale	on each side of the forehead, laterally from the elevation of the linea temporalis
Chk <sub>r</sub> , Chk <sub>i</sub>	cheek	at the intersection between Camper's plane and a line connecting the external eye canthus with the labial commissura
Zy <sub>r</sub> , Zy <sub>i</sub>	zygion	most lateral point of the zygomatic arch
Al <sub>r</sub> , Al <sub>i</sub>	alare	most lateral point on the alar contour
Ac <sub>r</sub> , Ac <sub>i</sub>	nasal alar crest	most lateral point in the curved base of nasal ala
ltn <sub>r</sub> , ltn <sub>i</sub>	inferior terminal of the nostril	inferior point of the nostril axis
Stn <sub>r</sub> , Stn <sub>i</sub>	superior terminal of the nostril	superior point of the nostril axis
Cph <sub>r</sub> , Cph <sub>i</sub>	crista philtri	on the elevated margin of the philtrum just above the vermilion line
Ch <sub>r</sub> , Ch <sub>i</sub>	cheilion	labial commissura
T <sub>r</sub> , T <sub>i</sub>	tragion	upper margin of the tragus
Go <sub>r</sub> , Go <sub>i</sub>	gonion	most lateral point on the mandibular angle
Pra <sub>r</sub> , Pra <sub>i</sub>	preaurale	most anterior point of the ear
Sa <sub>r</sub> , Sa <sub>i</sub>	superaurale	highest point on the auricle
Pa <sub>r</sub> , Pa <sub>i</sub>	postaurale	most posterior point on the auricle
Sba <sub>r</sub> , Sba <sub>i</sub>	subaurale	lowest point on the free margin of the auricle

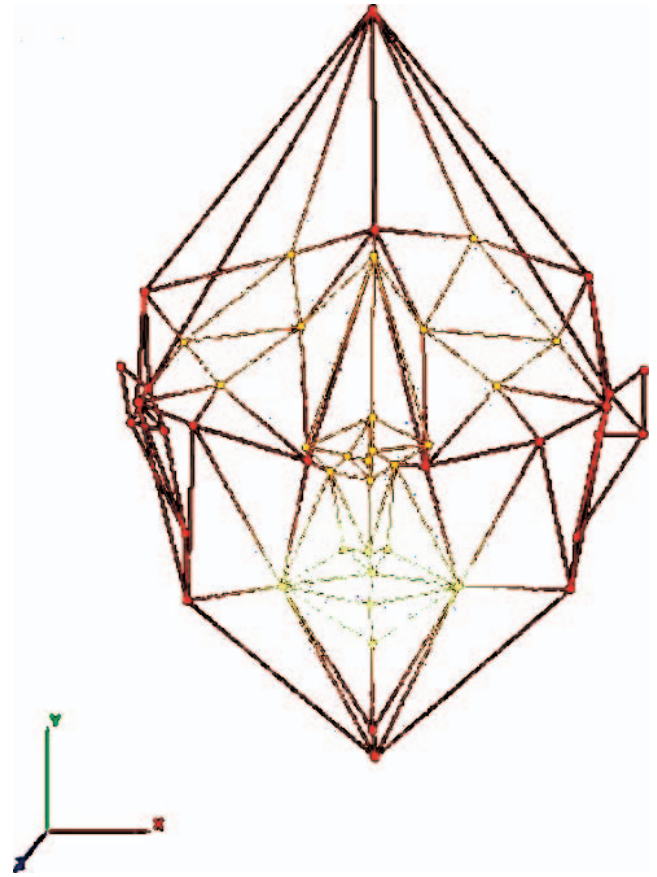


**Figure 2.** Geometric model obtained with 50 landmarks digitized by the electromagnetic three-dimensional tablet. Landmarks actually used for angles and distances are marked with a black dot.

**Table 2.** Analyzed Distances and Angles<sup>a</sup>

Distance	Angle
Ex <sub>r</sub> -Ex <sub>i</sub>	N-Sn-Pg
T <sub>r</sub> -T <sub>i</sub>	Sl-N-Sn
Go <sub>r</sub> -Go <sub>i</sub>	T <sub>r</sub> -N-T <sub>i</sub>
Ch <sub>r</sub> -Ch <sub>i</sub>	T <sub>r</sub> -Prn-T <sub>i</sub>
Tr-N	T <sub>r</sub> -Pg-T <sub>i</sub>
N-Sn	Ex <sub>r</sub> -N-Ex <sub>i</sub>
Sn-Pg	Go <sub>r</sub> -Pg-Go <sub>i</sub>
N-Pg	T <sub>r</sub> -Go <sub>r</sub> -Pg
N-(T <sub>r</sub> -T <sub>i</sub> )	T <sub>r</sub> -Go <sub>i</sub> -Pg
Sn-(T <sub>r</sub> -T <sub>i</sub> )	N-Prn-Pg
Pg-(T <sub>r</sub> -T <sub>i</sub> )	Sn-N-Prn
Pg-(Go <sub>r</sub> -Go <sub>i</sub> )	(T <sub>r</sub> -Al <sub>i</sub> )-(Go <sub>r</sub> -Pg)
Tr-Go	(T <sub>r</sub> -Al <sub>i</sub> )-(Go <sub>i</sub> -Pg)
Ls-(Prn-Pg)	(T <sub>r</sub> -N)-(Go <sub>r</sub> -Pg)
Li-(Prn-Pg)	Prn-Sn-Ls
	Li-Sl-Pg
	(Sn-Ls)-(Li-Pg)
	(Sn-Ls)-(Li-Sl)

<sup>a</sup> In subscripts: l, left side; r, right side.



**Figure 3.** Set of photographs taken at different angles.

angles (front, 3/4 right side, and 3/4 left side), while the subject maintained a natural head position. The three photographs were taken in approximately 3 minutes. Specific software assigned landmarks as assisted by PhotoModeler Pro, and as referenced in each picture. Subsequently, geometric models of the face were obtained for each subject and distances and angles were calculated.

We took subjects' pictures using a 6.0-mega pixel digital camera (Sony DSC-H2 Cybershot; Sony Corporation, Tokyo, Japan) positioned on a tripod at a fixed distance of 1.5 m. As specified by the PhotoModeler software, the system was calibrated with a set of standardized photographs of a guide paper (Figure 4). Reference paper marks were placed on the wall behind subjects to provide metric calibration.

After 1 month, we repeated the measurements on three subjects at random to verify the reproducibility of



**Figure 4.** Guide paper used for calibration of the photomodeler.

the photographic tracings, to reduce the potential for memory bias.

In addition, for analysis of reproducibility after repositioning, three new subjects were included in two different photographic sessions. Camera and subject positions were modified between photos and between replicate sets. For evaluation of the random error, the technical error of measurement (TEM) was computed.<sup>3,4,17</sup> When two measurements were used, TEM was computed as follows:

$$\text{TEM} = \sqrt{\sum D^2 / 2n}$$

where  $D$  is the difference between repeated measures and  $n$  is the number of analyzed individuals. To assess the systematic error between replicate measurements, paired  $t$ -tests with a 5% significance level ( $P > .05$ ) were performed.

### Statistical Analysis

Together with descriptive statistics (mean and standard deviation), the mean absolute difference (MAD) from the values of the electromagnetic digitizer and the photomodeler across each subject were calculated for all linear distances and angles. MAD is the average of absolute differences between the values of two sets of measurements.<sup>3,4</sup> We compared the data obtained with the two imaging systems using paired Student's  $t$ -tests and considered a  $P$  value of .05 or smaller to be significant.

### RESULTS

Among 15 linear measurements, two mean differences between measurements obtained via electro-

**Table 3.** Comparison Between Linear Distances Computed With the Photographic Method and the Electromagnetic Digitizer<sup>a</sup>

Distances	Electromagnetic Digitizer		Photo		MAD <sup>b</sup>	P Value <sup>c</sup>
	Mean	SD	Mean	SD		
Ex <sub>r</sub> -Ex <sub>i</sub>	90.5	5.23	91.12	5.69	0.62	.07 (ns)
T <sub>r</sub> -T <sub>i</sub>	141.85	7.92	144.52	7.54	2.67	.01*
Go <sub>r</sub> -Go <sub>i</sub>	116.16	9.23	117.78	7.91	1.62	.07 (ns)
Ch <sub>r</sub> -Ch <sub>i</sub>	47.13	5.1	47.81	5.97	0.68	.32 (ns)
Tr-N	67.44	7.99	67.03	8.52	0.41	.31 (ns)
N-Sn	53.23	3.71	52.95	3.7	0.28	.27 (ns)
Sn-Pg	57.13	3.75	56.75	4.05	0.38	.27 (ns)
N-Pg	108.43	5.87	108.35	6.12	0.08	.83 (ns)
N-(T <sub>r</sub> -T <sub>i</sub> )	98.59	4.59	97.9	4.55	0.69	.10 (ns)
Sn-(T <sub>r</sub> -T <sub>i</sub> )	107.84	5.82	106.83	6.22	1.01	.16 (ns)
Pg-(T <sub>r</sub> -T <sub>i</sub> )	125.48	8.84	122.96	9.08	2.52	.02*
Pg-Go	78.16	5.25	78.21	5.86	0.05	.95 (ns)
T-Go	64.98	7.58	63.41	7.65	1.57	.11 (ns)
Ls-(Prn-Pg)	5.62	1.55	5.64	1.47	0.02	.93 (ns)
Li-(Prn-Pg)	3.96	1.97	3.99	1.91	0.03	.91 (ns)

<sup>a</sup> All values are expressed in millimeters.

<sup>b</sup> MAD, Mean absolute differences.

<sup>c</sup> P values from paired *t*-tests comparing electromagnetic digitizer and photomodeler; ns indicates nonsignificant difference ( $P > .05$ ).

\* Statistically significant P value.

magnetic digitizer and photomodeler were significantly different from zero. MAD between measures was typically less than 1.62 mm, except for skull base width (T<sub>r</sub>-T<sub>i</sub>) and lower face depth (Pg-T) (Table 3).

Three of 18 analyzed angles showed statistically significant differences between the two techniques, revealing a discrepancy in facial convexity in the hori-

zontal plane (T<sub>r</sub>-N-T<sub>i</sub>, T<sub>r</sub>-Prn-T<sub>i</sub>, and T<sub>r</sub>-Pg-T<sub>i</sub> angles). Nevertheless, for these variables, the difference between means was smaller than 2 degrees, contrasting with the angle Ex<sub>r</sub>-N-Ex<sub>i</sub>, which presented an MAD of 2.51 degrees (Table 4).

We used TEM to analyze the random error in repeated digitizations of the photographs. Lower TEM values corresponded to more repeatable measurements. The highest values were noted for distances and angles involving the exocanthion (Ex), followed by angles including the gonion (Go) (Table 5). On no occasion were systematic errors found (all *t*-tests were not significant).

When the subjects and the camera moved among each set, all error values increased (Table 6), showing the highest values of 5.26 mm for linear measurements (T<sub>r</sub>-T<sub>i</sub>) and 5.61 degrees for angular measurements (T<sub>r</sub>-Go<sub>r</sub>-Pg). However, no systematic differences were found between replicate measurements ( $P > .05$ ).

## DISCUSSION

When craniofacial growth patterns or anatomic variations are described, conventional direct anthropometry currently is considered the gold standard for in vivo assessments: the method is simple, is low in cost, and does not require complex instrumentation.<sup>6,7,16</sup> Unfortunately, it is time consuming, it requires very well trained and experienced examiners, and it is very demanding for both the clinician and the patient.<sup>3,7,16</sup>

**Table 4.** Comparison Between Angles Computed Using the Photographic Method and the Electromagnetic Digitizer<sup>a</sup>

Angles	Electromagnetic Digitizer		Photo		MAD <sup>b</sup>	P Value <sup>c</sup>
	Mean	SD	Mean	SD		
N-Sn-Pg	159.07	3.71	159.45	3.86	0.38	.08 (ns)
Sl-N-Sn	12.05	1.76	11.87	2.03	0.18	.49 (ns)
T <sub>r</sub> -N-T <sub>i</sub>	71.04	2.96	72.56	2.95	1.52	.03*
T <sub>r</sub> -Prn-T <sub>i</sub>	60.23	2.14	62.04	2.69	1.81	.01*
T <sub>r</sub> -Pg-T <sub>i</sub>	58.92	2.36	60.43	3.02	1.51	.04*
Ex <sub>r</sub> -N-Ex <sub>i</sub>	116.20	5.37	118.71	6.43	2.51	.052 (ns)
Go <sub>r</sub> -Pg-Go <sub>i</sub>	73.66	3.24	74.19	3.05	0.53	.65 (ns)
T <sub>r</sub> -Go <sub>r</sub> -Pg	125.63	5.61	125.92	6.26	0.29	.67 (ns)
T <sub>r</sub> -Go <sub>r</sub> -Pg	124.74	4.97	124.67	5.67	0.07	.87 (ns)
N-Prn-Pg	126.59	3.11	127.17	3.53	0.58	.07 (ns)
Sn-N-Prn	21.70	1.59	21.35	1.65	0.35	.08 (ns)
(T <sub>r</sub> -Ala <sub>r</sub> )-(Go <sub>r</sub> -Pg)	11.52	1.87	11.79	2.58	0.27	.56 (ns)
(T <sub>r</sub> -Ala <sub>i</sub> )-(Go <sub>r</sub> -Pg)	9.98	2.91	9.69	2.5	0.29	.62 (ns)
(T-N)-(Go-Pg)	32.24	5.56	33.07	5.43	0.83	.11 (ns)
Prn-Sn-Ls	125.55	8.79	125.46	7.52	0.09	.95 (ns)
Li-Sl-Pg	132.74	11.93	133.56	11.43	0.82	.76 (ns)
(Sn-Ls)-(Li-Pg)	165.14	9.14	164.96	8.52	0.18	.92 (ns)
(Sn-Ls)-(Li-Sl)	140.54	15.95	140.55	12.21	0.01	1.00 (ns)

<sup>a</sup> All values are degrees.

<sup>b</sup> MAD, Mean absolute differences.

<sup>c</sup> P values from paired *t*-tests comparing electromagnetic digitizer and photomodeler; ns indicates nonsignificant difference ( $P > .05$ ).

\* Statistically significant P values.

**Table 5.** Error Analysis: Reproducibility of Tracings, Re-performed After 1 Month

Distances, mm	TEM <sup>a</sup> (n = 3)	P Value <sup>b</sup>	Angles, degrees	TEM <sup>a</sup> (n = 3)	P Value <sup>b</sup>
Ex <sub>r</sub> -Ex <sub>i</sub>	1.57	.07	N-Sn-Pg	0.25	.17
T <sub>r</sub> -T <sub>i</sub>	0.97	.51	SI-N-Sn	0.10	.17
Go <sub>r</sub> -Go <sub>i</sub>	0.23	.85	T <sub>r</sub> -N-T <sub>i</sub>	1.12	.62
Ch <sub>r</sub> -Ch <sub>i</sub>	0.74	.38	T <sub>r</sub> -Prn-T <sub>i</sub>	1.16	.48
Tr-N	0.25	.79	T <sub>r</sub> -Pg-T <sub>i</sub>	1.03	.35
N-Sn	0.55	.32	Ex <sub>r</sub> -N-Ex <sub>i</sub>	2.84	.16
Sn-Pg	0.29	.64	Go <sub>r</sub> -Pg-Go <sub>i</sub>	2.61	.24
N-Pg	0.13	.83	T <sub>r</sub> -Go <sub>r</sub> -Pg	1.05	.74
N-(T <sub>r</sub> -T <sub>i</sub> )	0.42	.64	T <sub>r</sub> -Go <sub>i</sub> -Pg	0.54	.97
Sn-(T <sub>r</sub> -T <sub>i</sub> )	0.23	.78	N-Prn-Pg	0.20	.37
Pg-(T <sub>r</sub> -T <sub>i</sub> )	0.28	.78	Sn-N-Prn	0.11	.18
Pg-Go	0.90	.68	(T <sub>r</sub> -Ala <sub>r</sub> )-(Go <sub>r</sub> -Pg)	1.45	.55
T-Go	0.19	.89	(T <sub>r</sub> -Ala <sub>r</sub> )-(Go <sub>i</sub> -Pg)	1.14	.38
Ls-(Prn-Pg)	0.50	.51	(T-N)-(Go-Pg)	0.59	.15
Li-(Prn-Pg)	0.21	.28	Prn-Sn-Ls	0.72	.18
			Li-SI-Pg	2.02	.72
			(Sn-Ls)-(Li-Pg)	2.10	.66
			(Sn-Ls)-(Li-SI)	1.92	.34

<sup>a</sup> TEM, Technical error of measurement.

<sup>b</sup> P values from paired *t*-tests comparing repeated digitizations. All P values are not significant ( $P > .05$ ).

Therefore, the use of 3D imaging systems is growing, with several clinical applications available for diagnosis, presurgical planning, postsurgical outcome assessment, and syndrome identification.

A number of relatively noninvasive methods for 3D imaging have been developed over past decades to obtain facial anthropometric data.<sup>1,3-5,8,11-13,19,21-24</sup> Unfortunately, the cost and complexity of these methods often limit their use to research facilities.

In the current study, a simple, low-cost, noninvasive 3D method for facial surface measurements was developed and tested. It eliminates the need for direct contact with the subject, thereby avoiding displace-

ment/deformation of soft tissues.<sup>3,14,24</sup> The investigator can use coordinates of the landmarks for off-line calculation of distances and angles. Anyone can evaluate a new measurement from the same landmarks without new data collection.<sup>22</sup>

When compared with the electromagnetic digitizer,<sup>22</sup> the current 3D system (Photomodeler) can be seen to have both advantages and limitations. In both methods, facial landmarks should be identified and marked on the face of each subject before digitization/photographic recording.<sup>3,4,16</sup> Subsequently, landmarks are digitized on-line when the electromagnetic instrument is used, and off-line when the photographic system is

**Table 6.** Error Analysis: Reproducibility During Subject Rearrangement

Distances, mm	TEM <sup>a</sup> (n = 3)	P Value <sup>b</sup>	Angles, degrees	Error (n = 3)	P Value <sup>b</sup>
Ex <sub>r</sub> -Ex <sub>i</sub>	3.91	.13	N-Sn-Pg	1.52	.53
T <sub>r</sub> -T <sub>i</sub>	5.26	.20	SI-N-Sn	0.82	.49
Go <sub>r</sub> -Go <sub>i</sub>	3.24	.19	T <sub>r</sub> -N-T <sub>i</sub>	4.02	.95
Ch <sub>r</sub> -Ch <sub>i</sub>	2.39	.26	T <sub>r</sub> -Prn-T <sub>i</sub>	3.76	.87
Tr-N	1.11	.64	T <sub>r</sub> -Pg-T <sub>i</sub>	3.03	.84
N-Sn	1.09	.43	Ex <sub>r</sub> -N-Ex <sub>i</sub>	5.14	.46
Sn-Pg	2.70	.07	Go <sub>r</sub> -Pg-Go <sub>i</sub>	4.41	.73
N-Pg	3.86	.15	T <sub>r</sub> -Go <sub>r</sub> -Pg	3.63	.31
N-(T <sub>r</sub> -T <sub>i</sub> )	3.65	.46	T <sub>r</sub> -Go <sub>i</sub> -Pg	4.26	.34
Sn-(T <sub>r</sub> -T <sub>i</sub> )	2.02	.75	N-Prn-Pg	3.08	.73
Pg-(T <sub>r</sub> -T <sub>i</sub> )	2.58	.65	Sn-N-Prn	0.71	.44
Pg-Go	3.53	.42	(T <sub>r</sub> -Ala <sub>r</sub> )-(Go <sub>r</sub> -Pg)	1.77	.18
T-Go	0.48	.78	(T <sub>r</sub> -Ala <sub>r</sub> )-(Go <sub>i</sub> -Pg)	1.67	.86
Ls-(Prn-Pg)	0.31	.61	(T-N)-(Go-Pg)	2.27	.57
Li-(Prn-Pg)	0.99	.21	Prn-Sn-Ls	4.22	.34
			Li-SI-Pg	5.58	.16
			(Sn-Ls)-(Li-Pg)	0.67	.38
			(Sn-Ls)-(Li-SI)	5.61	.12

<sup>a</sup> TEM, Technical error of measurement.

<sup>b</sup> P values from paired *t*-tests comparing repeated photographic sets. All P values are not significant ( $P > .05$ ).

used. The photographic system allows digitization of an unlimited number of landmarks, but the number of landmarks digitized by the electromagnetic instrument should represent a compromise between sufficiently detailed individuation of the anatomic characteristics of the face and digitization time.<sup>16</sup>

The photomodeler system uses a picture set as a reference for making the triangulation. Generally, we used frontal pictures as a reference. Consequently, we found the main problem of this system seemed to be marker location, at which point it is impossible to assign some landmarks in the reference pictures. One of the indistinguishable landmarks often happened to be tragus (T). This may explain the results obtained in this study, which showed significant differences when compared with the reference method in two linear measures ( $T_r-T_i$ ; Pg-T) and in three angles ( $T_r-N-T_i$ ;  $T_r-Prn-T_i$ ;  $T_r-Pg-T_i$ ); all of these variables involve tragus (T). Indeed, we found that the data acquisition system was best used for different facial morphologies and dimensions. The ears often are digitized with some difficulty even when complex stereophotographic and laser scanning instruments are used,<sup>8,11,12,21</sup> and similar method errors have been reported with the tragus landmark.<sup>4</sup>

The literature includes frequent reports of MAD as a precision estimate,<sup>3,4</sup> because it affords easy interpretation and is calculated simply. Current anthropometric literature<sup>10</sup> usually considers less than 1 mm acceptable. We surpassed this threshold only by four distances out of 15, and by four angles out of 18 in the current study. The greatest variations were seen in distances, including the tragus and gonion landmarks, and in angles of facial convexity on the horizontal plane, which crossed both facial halves. This result is consistent with that of Weinberg et al<sup>4</sup> and can be explained by the difficulty of assigning lateral landmarks in reference photos. For the "Ex" landmarks, two factors should be considered: in some cases, noncorrect identification caused by the eyelashes; in other cases, lack of previous identification with a black mark. Indeed, the previous marking significantly reduces method error with both contact and optical digitizers.<sup>3,4,22</sup>

Furthermore, the presence of hairs may mask some landmarks, resulting in missed landmarks<sup>24</sup> or the non-identification of some points in all three photos. In this case, after analyzing and processing all evident landmarks, the software gave us an approximated location of the missed landmark in all pictures to complete the geometric 3D reconstruction. Thus, good pictures with fine resolution are required to minimize error. The good performance of profile distances and angles is consistent with previous investigations that compared photographs vs classic anthropometry.<sup>7</sup> Indeed, profile

landmarks all belong to a single plane, thus minimizing projection errors. Additionally, they are easy to identify in well-made photographs.

The reproducibility of the 3D computerized electromagnetic digitizer throughout landmark identification and marker positioning was reported previously.<sup>22</sup> According to anthropometric literature,<sup>3,4</sup> the technical error of measurement was included in this study to verify the reproducibility of the photomodeler system. The greatest method error for linear measures (distances) between first and second digitization of the same set of photographs was 1.57 mm for the  $Ex_r-Ex_i$  distance, without significant systematic differences. Therefore, the results indicate acceptable repeatability for landmark digitization. Similarly, for angular measurements, the differences were always lower than 3 degrees, and differences larger than 2 degrees were observed in only four angles ( $Ex_r-N-Ex_i$ ;  $Go_r-Pg-Go_i$ , Li-SI-Pg; and [Sn-Ls]-[Li-Pg]). This outcome is consistent with that of Weinberg et al,<sup>4</sup> who reported that the estimation of error magnitude tended to be greater in variables containing difficult-to-see landmarks and variables crossing the labial fissure.

The photomodeler system takes three photographs of each set in different moments and angles, and possible movement of the head may occur. Therefore, we evaluated its influence on data collection during subject and camera relocation. Increased errors were observed, with TEM up to 5.3 mm ( $T_r-T_i$  distance) and 5.6 degrees (angles Li-SI-Pg and Sn-Ls-Li-SI).

Notwithstanding the lack of bias (systematic errors), these differences are of clinical importance and indicate that lip (landmark SI is included in both angles with the largest error), eye (landmark Ex), and ear (landmark T) positions are most critical in repeated photographs.<sup>15</sup>

For reduction in measurement error, photographs may be obtained simultaneously with the use of three cameras, but this would increase the monetary cost of the analysis. More simply, subjects should avoid making head movements during photo acquisition. Nevertheless, the method is less demanding than classical anthropometry, especially for children, and it can be coupled with conventional radiographs to allow repeated measurements during treatment and follow-up.<sup>7,13,22</sup>

In summary, the photographic system described in the current investigation can be used to measure facial characteristics with a satisfactory degree of repeatability, but some landmarks need to be reevaluated, thereby improving the acquisition. Additional studies should be undertaken to improve the protocol and enhance the accuracy of the method.

## CONCLUSIONS

- The three-dimensional photogrammetry system tested in the present study can assess the coordinates of facial landmarks with satisfactory precision and can be used to obtain reliable facial measurements.
- The method is relatively fast and inexpensive equipment is needed; thus it is simple for those in private practice, researchers, or other practitioners to use.<sup>7,9,15</sup>
- Photomodeler system measurements can be used to assess linear distances and angles.

## REFERENCES

1. Ghoddousi H, Edler R, Haers P, Wertheim D, Greenhill D. Comparison of three methods of facial measurement. *Int J Oral Maxillofac Surg.* 2007;36:250–258.
2. Tollefson TT, Sykes JM. Computer imaging software for profile photograph analysis. *Arch Facial Plast Surg.* 2007;9:113–119.
3. Wong JY, Oh AK, Ohta E, Hunt AT, Rogers GF, Mulliken JB, Deutsch CK. Validity and reliability of craniofacial anthropometric measurement of 3D digital photogrammetric images. *Cleft Palate Craniofac J.* 2008;45:232–239.
4. Weinberg SM, Scott NM, Neiswanger K, Brandon CA, Marazita ML. Digital three-dimensional photogrammetry: evaluation of anthropometric precision and accuracy using a Genex 3D camera system. *Cleft Palate Craniofac J.* 2004;41:507–518.
5. Weinberg SM, Naidoo S, Govier DP, Martin RA, Kane AA, Marazita ML. Anthropometric precision and accuracy of digital three-dimensional photogrammetry: comparing the Genex and 3dMD imaging systems with one another and with direct anthropometry. *J Craniofac Surg.* 2006;17:477–483.
6. Braddock SR, Henley KM, Maria BL. The face of Joubert syndrome: a study of dysmorphology and anthropometry. *Am J Med Genet.* 2007;143A:3235–3242.
7. Guyot L, Dubuc M, Richard O, Philip N, Dutour O. Comparison between direct clinical and digital photogrammetric measurements in patients with 22q11 microdeletion. *Int J Oral Maxillofac Surg.* 2003;32:246–252.
8. Hammond P. The use of 3D face shape modeling in dysmorphology. *Arch Dis Child.* 2007;92:1120–1126.
9. Dimaggio FR, Ciusa V, Sforza C, Ferrario VF. Photographic soft-tissue profile analysis in children at 6 years of age. *Am J Orthod Dentofacial Orthop.* 2007;132:475–480.
10. Douglas TS. Image processing for craniofacial landmark identification and measurement: a review of photogrammetry and cephalometry. *Comput Med Imaging Graph.* 2004;28:401–419.
11. Hammond P, Hutton TJ, Allanson JE, et al. 3D analysis of facial morphology. *Am J Med Genet.* 2004;126A:339–348.
12. Kau CH, Richmond S, Zhurov AI, Knox J, Chestnutt I, Hartles F, Playle R. Reliability of measuring facial morphology with a 3-dimensional laser scanning system. *Am J Orthod Dentofacial Orthop.* 2005;128:424–430.
13. Sforza C, Peretta R, Grandi G, Ferronato G, Ferrario VF. Three-dimensional facial morphometry in skeletal Class III patients: a non-invasive study of soft-tissue changes before and after orthognathic surgery. *Br J Oral Maxillofac Surg.* 2007;45:138–144.
14. Muradin MS, Rosenberg A, van der Bilt A, Stoelinga PJ, Kooze R. The reliability of frontal facial photographs to assess changes in nasolabial soft tissues. *Int J Oral Maxillofac Surg.* 2007;36:728–734.
15. Sforza C, Dimaggio FR, Dellavia C, Grandi G, Ferrario VF. Two-dimensional vs three-dimensional assessment of soft tissue facial profile: a non invasive study in 6-year-old healthy children. *Minerva Stomatol.* 2007;56:253–265.
16. Sforza C, Ferrario VF. Soft-tissue facial anthropometry in three dimensions: from anatomical landmarks to digital morphology in research, clinics and forensic anthropology. *J Anthropol Sci.* 2006;84:97–124.
17. Vander Pluym J, Shan WW, Taher Z, Beaulieu C, Plewes C, Peterson AE, Beattie OB, Bamforth JS. Use of magnetic resonance imaging to measure facial soft tissue depth. *Cleft Palate Craniofac J.* 2007;44:52–57.
18. Loukas M, Kapos T, Louis RG Jr, Wartman C, Jones A, Hallner B. Gross anatomical, CT and MRI analyses of the buccal fat pad with special emphasis on volumetric variations. *Surg Radiol Anat.* 2006;28:254–260.
19. Khambay B, Nairn N, Bell A, Miller J, Bowman A, Ayoub AF. Validation and reproducibility of a high-resolution three-dimensional facial imaging system. *Br J Oral Maxillofac Surg.* 2008;46:27–32.
20. Kimoto K, Garrett NR. Evaluation of a 3D digital photographic imaging system of the human face. *J Oral Rehabil.* 2007;34:201–205.
21. Winder RJ, Darvann TA, McKnight W, Magee JD, Ramsay-Baggs P. Technical validation of the Di3D stereophotogrammetry surface imaging system. *Br J Oral Maxillofac Surg.* 2008;46:33–37.
22. Ferrario VF, Sforza C, Poggio CE, Cova M, Tartaglia G. Preliminary evaluation of an electromagnetic three-dimensional digitizer in facial anthropometry. *Cleft Palate Craniofac J.* 1998;35:9–15.
23. Ferrario VF, Sforza C, Serrao G, Ciusa V, Dellavia C. Growth and aging of facial soft tissues: a computerized three-dimensional mesh diagram analysis. *Clin Anat.* 2003;16:420–433.
24. Majid Z, Chong AK, Ahmad A, Setan H, Samsudin AR. Photogrammetry and 3D laser scanning as spatial data capture techniques for a national craniofacial database. *Photogramm Rec.* 2005;20:48–68.